

Synthesis of efficient ZnO-based random lasing medium using laser-induced air breakdown processing

A. V. Kabashin^{a)} and A. Trudeau

Laser Processing Laboratory, Department of Engineering Physics, Ecole Polytechnique de Montréal, Case Postale 6079, Succ. Centre-ville, Montréal, Québec, Canada H3C 3A7

W. Marine

CRMCN UPR CNRS 7251, Département de Physique, Case 901 Faculté des Sciences de Luminy, 13288 Marseille, Cedex 9, France

M. Meunier^{b)}

Laser Processing Laboratory, Department of Engineering Physics, Ecole Polytechnique de Montréal, Case Postale 6079, Succ. Centre-ville, Montréal, Québec, Canada H3C 3A7

(Received 16 July 2007; accepted 22 October 2007; published online 13 November 2007)

A simple local patterning laser-assisted method to transform bulk metallic Zn into a highly efficient ZnO-based random lasing medium is reported. The method uses the plasma of CO₂ laser-induced air breakdown to treat the surface of a Zn target and thus transform it into a porous, nanostructured ZnO layer, which exhibits a strong exciton photoluminescence band in the UV (380 nm). We show that the synthesized ZnO-based material can work as an efficient random lasing medium, simultaneously strongly scattering and amplifying pumping light, leading to a mirrorless generation of few laser emission narrow (<0.5 nm) lines within the exciton band. © 2007 American Institute of Physics.

[DOI: 10.1063/1.2809606]

Random lasing is an interesting physical phenomenon that offers attractive opportunities for the development of optoelectronics devices and components.^{1–13} This phenomenon can arise under a simultaneous high scattering and gain in some highly disordered media.¹⁴ When the scattering mean free path becomes equal or less than a wavelength, photon may return to the scattering center from where it originated, forming closed loop paths. If the amplification along such a path exceeds the loss, laser oscillation can arise in the loop, which serves as a laser resonator. In this case, the phase shift along the loop must be equal to a multiple of 2π . Unlike the traditional semiconductor lasers, which have well-defined cavities, the random laser cavities are “self-formed” due to a strong optical scattering in polycrystalline films. Random lasing-related effects have been demonstrated in different media including semiconductor-based colloidal nanoparticles,¹ powders,^{2–5} thin films,^{6–10} conjugated polymer films,¹¹ suspensions containing laser dyes, and metal nanoparticles.^{12,13}

With an extremely efficient direct band gap transition at 3.37 eV and the exciton binding energy exceeding 60 meV, ZnO is considered as one of most efficient materials for the implementation of random lasing effect. Normally, high scattering in ZnO medium requires the production of subwavelength crystals with their good relative separation.¹⁵ The basic material is obtained by the deposition of already formed ZnO polycrystalline powders³ or ZnO-based films on some substrates (sapphire, silica, silicon)^{5–9} and the desired nanostructures are achieved by either heating the substrate during the deposition^{4,10} or by a postfabrication annealing of already formed films.^{5–9} In the latter case, the thermal treatment leads to the formation of submicron crystals with lateral facets separating the crystals from each other. In all cases, random lasing effect is observed as 0.3 nm width narrow laser

lines appear within the exciton-based emission band normally centered around 380–385 nm. Despite relative elaboration of these above-stated approaches, alternative low-cost methods for the fabrication of ZnO-based random lasing medium are still in need.

In this letter, we report a simple, low-cost laser-assisted method for the fabrication of such medium from a bulk piece of metal in normal ambient conditions. The method uses the phenomenon of laser-induced air breakdown¹⁶ to locally treat a Zn target. As we previously showed, the same phenomenon can be used to locally pattern nanostructured photoluminescent Si-based structures on a Si wafer.^{17–20}

In the experiments, we used a pulsed TEA CO₂ laser (wavelength of 10.6 μm , pulse energy of 1 J, pulse length of 1 μs full width at half maximum, and repetition rate of 3 Hz). The radiation was focused by a Fresnel lens with a focal length of 5 cm, giving the radiation intensity of about 10⁸ W/cm² at the focal plane, while the irradiation spot represented a rectangular area with dimensions of about 1.5 \times 1 mm². Typical fluences used were between 0.14 and 0.4 J/cm². Standard targets of metallic Zn (purity of 99.995%) with dimensions about 1 \times 1 cm² were used as targets. Experiments were carried out in atmospheric air (1 atm, 20 °C, and 40% humidity). Photoluminescence (PL) spectra were recorded on an Acton 500i spectrometer coupled with a rapid intensified charge coupled device camera using a 100 fs pulsed laser excitation at 355 nm. Field emission scanning electron microscopy (SEM) (JEOL 6320F) was used to examine structural properties of the films. The crystalline structure of the films was obtained by x-ray diffraction (XRD) spectroscopy (X'pert XRD system, Philips Corp). In addition, x-ray photoemission spectroscopy (XPS) was used to determine surface layer composition.

Focusing the radiation on a Zn target led to the formation of a laser-induced air breakdown plasma, which was observed as a bright flash, moving from the target toward the focusing lens. After the breakdown initiations by one to five

^{a)}Electronic mail: andrei.kabashin@polymtl.ca

^{b)}Electronic mail: michel.meunier@polymtl.ca

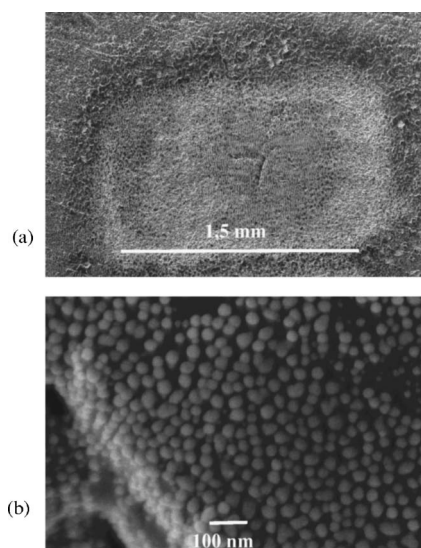


FIG. 1. Typical SEM images at different magnifications of a Zn target surface processed under 100 air breakdown initiations.

laser pulses, a gray-tint area was formed under the focal spot on the target surface. Figure 1(a) shows a SEM image of the whole treated area of a typical processed sample. One can see that the size of the treated area correlated with the size of the spot and that the treatment did not lead to a redeposition of material around the irradiation spot or to the formation of micron-scale spikes within the irradiation spot, as it takes place in conventional laser ablation by nanosecond ultraviolet^{19,21} or femtosecond²² radiation. Furthermore, the crater, which is typically formed under the irradiation spot during the laser ablation, was essentially absent. In contrast, as shown in Fig. 1(b), the treated area was rather formed by a highly porous material composed of nanoscale spheres of dimension around 25–50 nm. These spheres were densely packed forming a “photon-crystal-like structure.” The treatment by thousands of pulses could also lead to a coagulation of these nanospheres and the formation of few microns in size “cauliflower” structures.

XPS studies confirmed the formation of ZnO layer on the Zn substrate, which was illustrated by the presence of zinc $2p\ 3/2$ and oxygen $1s$ peaks. The treatment led to the shift of Zn $2p\ 3/2$ peak from 1022 to 1021.4 eV and of the oxygen $1s$ peak from 531.8 to 529.9 eV, suggesting a transformation of surface layer from naturally surface-oxidized Zn to pure ZnO. The treatment led to a drastic decrease of carbon content, associated with the removal of initial contaminants from the surface, and the increase of Zn/O ratio. Not exceeding 0.24 for initial zinc samples, such a ratio reached the factor of 1 when the target was treated at relatively high fluences ($>0.2\ \text{J}/\text{cm}^2$). The presence of a strong (002) peak at $2\theta=34.4^\circ$ in XRD spectra suggested the presence of submicron ZnO crystals with a wurzite structure having their c axis normal to the substrate plane. As shown in Fig. 2, the increase of laser shots led to the increase of intensity of this line and appropriate decrease of its width at half maximum, normally associated with a relative increase of the nanocrystal size with the number of laser shots. It is known^{23,24} that the broadness of XRD peaks is mainly determined by clusters of the smallest crystals in the deposit. As the instrumental noise is relatively low, this property could be used to estimate with a fair accuracy (see, e.g., Ref. 19) the minimal crystal size in the deposit by the Debye-Scherrer

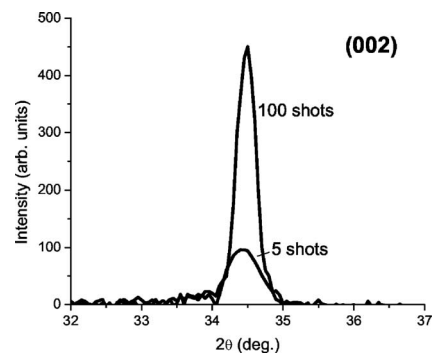


FIG. 2. Typical highly resolved x-ray diffraction pattern near the (0-0-2) line from a Zn target.

formula.¹⁸ Taking the broadness of a typical ZnO peak from a highly resolved XRD spectrum $2\theta=0.28^\circ$, the estimation gives a minimal grain size of about 35 nm, which is in excellent agreement with the size of nanospheres shown in Fig. 1(b).

The processed area exhibited PL signals, which could be easily seen by naked eyes. Photoluminescence spectra from typical samples were characterized by the domination of a strong and narrow exciton-related band centered at 380–385 nm, as shown in Fig. 3(a). The additional defect-related band in the yellow-green range, whose intensity was weaker by more than one order of magnitude, completely disappeared when the processing fluence was increased above $0.3\ \text{J}/\text{cm}^2$. As shown in Fig. 3(b), a detailed examination of the spectra revealed the appearance of extremely narrow (0.3–0.5 nm full width at half maximum) lines within the exciton-related band. Further increase of the excitation pumping intensity to $4 \times 10^5\ \text{W}/\text{cm}^2$ gave rise to the appearance of additional lines [Fig. 3(c)]. Normally, the generation of such lines is attributed to the random lasing effect, as it was observed with samples prepared through a deposition of already formed ZnO polycrystalline powders³ or thermally treated/annealed ZnO-based films.^{4–10} Note that such efficient production of random lasing medium through one simple and rapid step from a bulk piece of Zn is a pleasant surprise, taking into account the extreme simplicity of the fabrication method and of experimental conditions used (ambient air). Furthermore, the threshold of random lasing effect ($2.7 \times 10^5\ \text{W}/\text{cm}^2$) was comparable with lowest reported threshold values,^{3–9} promising a future implementation of random laser devices.

Thus, laser-induced air breakdown processing lead to an efficient synthesis of random lasing medium, while conventional laser ablation was unable to produce this medium without additional annealing steps. We reason that such difference of laser-assisted treatments is due to rather different mechanisms and conditions of material transformation in these two cases. In laser ablation, the radiation is mainly absorbed by the target, leading to a rapid release and cooling of ablated species under their interaction with the environment, thus preventing the formation of the required nanostructure and stoichiometry. In contrast, the breakdown processing is characterized by a strong photon absorption by the plasma itself.^{25,26} After the initial electron generation from the target, the formed plasma develops in the cold gas toward the focusing lens and absorbs the main IR radiation power at its shock wave forefront through the inverse bremsstrahlung mechanism. As a result, the plasma gets heated up to tem-

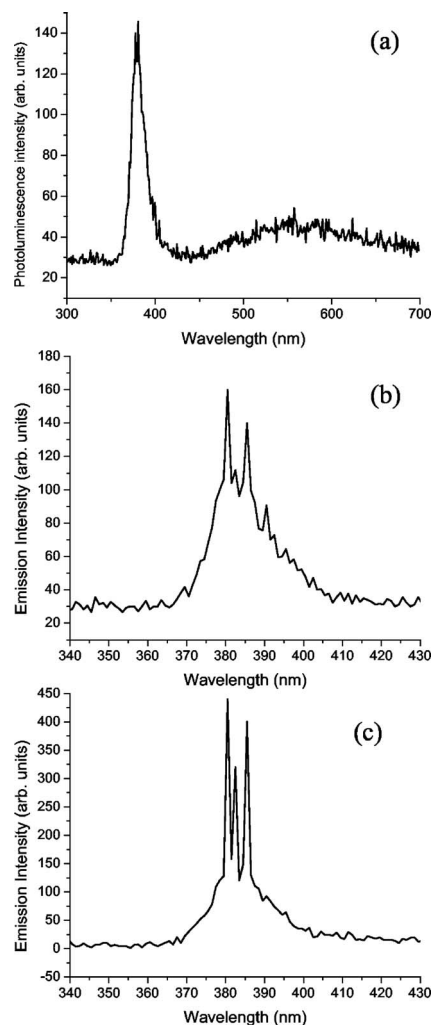


FIG. 3. (a) Typical survey photoluminescence spectrum from ZnO nanoparticles formed after the breakdown processing of a Zn target in air. The excited 100 fs pumping laser intensity at 355 nm was 3.0×10^5 W/cm². [(b) and (c)] High resolution PL spectra near the exciton emission band of processed samples measured under the excited pumping laser intensities of (b) 3.5×10^5 W/cm² and (c) 4×10^5 W/cm².

peratures of about 10^4 K, while the radiation power on the target surface decreases dramatically and the radiation-related ablation of material drops.²⁶ After the laser pulse, the plasma decays gradually during milliseconds containing intense currents (with magnitudes up to 10^6 A)²⁷ and various electromagnetic effects.^{28–30} The action of radiation probably leads to a localized melting and even flash evaporation of the target material in some casual points. The laser-ablated material and the upper target layer are then heated by the hot CO₂ laser-induced breakdown plasma or its currents during milliseconds, leading to both additional phase transformations and the initiation of chemical reactions in the “plasma reactor.” Since the radiation is pulsed at 3 Hz, one can assume recrystallization or local vapor redeposition of the material during the off times. The breakdown processing combines surface nanostructuring and material heating, giving rise to a desirable modification of ZnO-based structures. This double action is probably the main feature which differentiates the breakdown processing from conventional laser ablation.

In summary, we report a method for an effective and rapid formation of ZnO-based random lasing medium from a bulk piece of Zn using laser-induced air breakdown process-

ing. The produced layers exhibited defect-free emission of exciton-based band with narrow lines associated with random lasing effect. Due to its extreme simplicity and cost efficiency, the proposed method can be of importance for low-cost local patterning of random lasing components for optoelectronics applications. In this case, we imply the formation of nanostructured ZnO on a Zn plate or a preliminary deposited Zn film, whereas random lasing lines can be excited both optically and electrically. Although the latter electroluminescence-based approach yet requires additional research and confirmation, it promises the fabrication of practical low-cost and compact laser devices/components.

The authors acknowledge the financial contribution from the Natural Science and Engineering Research Council of Canada.

- ¹N. M. Lawandy, R. M. Balachandran, A. S. L. Gomes, and E. Sauvain, *Nature (London)* **368**, 436 (1994).
- ²D. S. Wiersma, M. P. Van Albada, and A. Lagendijk, *Phys. Rev. Lett.* **75**, 1739 (1995).
- ³H. Cao, Y. G. Zhao, H. C. Ong, S. T. Ho, J. Y. Dai, J. Y. Wu, and R. P. H. Chang, *Appl. Phys. Lett.* **73**, 3656 (1998).
- ⁴H. Cao, Y. G. Zhao, S. T. Ho, E. W. Seelig, Q. H. Wang, and R. P. H. Chang, *Phys. Rev. Lett.* **82**, 2278 (1999).
- ⁵Z. K. Tang, G. K. L. Wong, P. Yu, M. Kawasaki, A. Ohtomo, H. Koinuma, and Y. Segawa, *Appl. Phys. Lett.* **72**, 3270 (1998).
- ⁶H. C. Ong, J. Y. Dai, A. S. K. Li, G. T. Du, R. P. H. Chang, and S. T. Ho, *J. Appl. Phys.* **90**, 1663 (2001).
- ⁷C. Yuen, S. F. Yu, E. S. P. Leong, H. Y. Yang, S. P. Lau, and H. H. Hng, *IEEE J. Quantum Electron.* **41**, 970 (2005).
- ⁸H. D. Li, S. F. Yu, S. P. Lau, and E. S. P. Leong, *Appl. Phys. Lett.* **89**, 021110 (2006).
- ⁹S. F. Yu, C. Yuen, S. P. Lau, and H. W. Lee, *Appl. Phys. Lett.* **84**, 3244 (2004).
- ¹⁰E. V. Chelnokov, N. Bityurin, I. Ozerov, and W. Marine, *Appl. Phys. Lett.* **89**, 171119 (2006).
- ¹¹S. V. Frolov, W. Gellerman, M. Ozaki, K. Yoshino, and Z. V. Vardeny, *Phys. Rev. Lett.* **78**, 729 (1997).
- ¹²G. D. Dice, S. Mujumdar, and A. Y. Elezzabi, *Appl. Phys. Lett.* **86**, 131105 (2005).
- ¹³O. Popov, A. Zilbershtein, and D. Davidov, *Appl. Phys. Lett.* **89**, 191116 (2006).
- ¹⁴D. S. Wiersma and A. Lagendijk, *Phys. Rev. E* **54**, 4256 (1996).
- ¹⁵U. Ozgur, Y. I. Alilov, C. Liu, A. Teke, M. A. Reshnikov, S. Dogan, V. Avrutin, S.-J. Cho, and H. Morkoc, *J. Appl. Phys.* **98**, 041301 (2005).
- ¹⁶F. V. Bunkin, V. I. Konov, A. M. Prokhorov, and V. B. Fedorov, *JETP Lett.* **9**, 371 (1969).
- ¹⁷A. V. Kabashin and M. Meunier, *Appl. Surf. Sci.* **186**, 578 (2002).
- ¹⁸A. V. Kabashin and M. Meunier, *Appl. Phys. Lett.* **82**, 1619 (2003).
- ¹⁹A. V. Kabashin and M. Meunier, *Mater. Sci. Eng., B* **101**, 60 (2003).
- ²⁰D.-Q. Yang, A. V. Kabashin, V.-G. Pilon-Marien, E. Sacher, and M. Meunier, *J. Appl. Phys.* **95**, 5722 (2004).
- ²¹A. J. Pedraza, J. D. Fowlkes, and D. H. Lowndes, *Appl. Phys. Lett.* **74**, 2322 (1999).
- ²²T.-H. Her, R. J. Finlay, C. Wu, S. Deliwala, and E. Mazur, *Appl. Phys. Lett.* **73**, 1673 (1998).
- ²³B. D. Cullity, *Elements of X-ray Diffraction* (Addison-Wesley, Reading, MA, 1978), p. 81.
- ²⁴E. Bardet, J. E. Bouree, M. Cuniot, J. Dixmier, P. Elkaim, J. Le Duigou, A. R. Middya, and J. Perrin, *J. Non-Cryst. Solids* **198-200**, 867 (1996).
- ²⁵Yu. P. Raizer *Laser-Induced Discharge Phenomena* (Consultants Bureau, New York, 1977), p. 17.
- ²⁶A. M. Prokhorov, V. I. Konov, I. Ursu, and I. N. Mikhailescu, *Laser Heating of Metals* (Hilger, Bristol, 1990), p. 143.
- ²⁷M. G. Drouet and H. Pepin, *Appl. Phys. Lett.* **28**, 426 (1976).
- ²⁸V. V. Korobkin and R. V. Serov, *Pis'ma Zh. Eksp. Teor. Fiz.* **4**, 103 (1966) [*JETP Lett.* **4**, 70 (1966)].
- ²⁹A. V. Kabashin and P. I. Nikitin, *Quantum Electron.* **27**, 536 (1997).
- ³⁰A. V. Kabashin, P. I. Nikitin, W. Marine, and M. Sentis, *Appl. Phys. Lett.* **73**, 25 (1998).